crystals

MDPI

Article

Bond Behavior of Recycled Fiber Recycled Concrete with Reinforcement after Freeze-Thaw Cycles

Yu Liu [1], Jinghai Zhou [1,*], Di Wu [1], Tianbei Kang [1] and Aixia Liu [2]

[1] School of Civil Engineering, Shenyang Jianzhu University, Shenyang 110168, China; liuyu@stu.sjzu.edu.cn (Y.L.); sjzuwudi@163.com (D.W.); kangtianbei@sjzu.edu.cn (T.K.)
[2] Department of Civil Engineering, Shenyang Urban Construction University, Shenyang 110168, China; laixia1030@163.com
* Correspondence: zhoujinghai@sjzu.edu.cn; Tel.: +86-139-0405-7590

Abstract: Freeze-thaw (F-T) damage is the major factor destroying the bond behavior of reinforced concrete in the cold areas of China. The bond behavior between recycled fiber recycled concrete (RFRC) and reinforcement after F-T cycles was investigated in this paper. The pull-out tests were undertaken with the replacement rate (0, 50%, and 100%) of recycled aggregates (RA) and volume content (0, 0.12%, and 0.24%) of recycled fibers (RFs) as test variables. The results demonstrate that the F-T cycles will reduce the bond strength between RFRC and reinforcement. Bond strength decreases by 69.41% after 150 cycles. Moreover, RF can improve the bond strength between RFRC and reinforcing steel. Bonding strength increases by 11.35% with the addition of 0.12% RF. A simplified two-phase bond-slip model between RFRC and reinforced steel after F-T cycles was eventually established, and it correlated well with the experimental results. This research presents a theoretical basis for the application of RFRC in building structures in cold areas.

Keywords: bond behavior; freeze-thaw cycles; recycled fiber recycled concrete; bond strength; bond-slip

Citation: Liu, Y.; Zhou, J.; Wu, D.; Kang, T.; Liu, A. Bond Behavior of Recycled Fiber Recycled Concrete with Reinforcement after Freeze-Thaw Cycles. *Crystals* **2021**, *11*, 1506. https://doi.org/10.3390/cryst11121506

Academic Editors: Yu Wang, José L. García, Tomasz Sadowski, Amjad Albayati and Jian Geng

Received: 30 October 2021
Accepted: 1 December 2021
Published: 3 December 2021

1. Introduction

The booming construction industry has accelerated the consumption of natural resources, while generating huge amounts of construction and demolition waste (C&DW) [1]. According to statistics, each year, on a global scale, over 1.5 billion tons of C&DW are produced, of which, nearly 700 million tons are in China, as shown in Figure 1a, and this number keeps growing [2]. Such a huge amount of C&DW-occupied land, as seen in Figure 1b, pollutes air and water resources as well [3]. Not only is this a problem for China, but it is also a global problem [4]. Therefore, specialists from various countries actively explore the treatment of recycling mode of C&DW [5,6], research on the performance of recycled concrete (RC), and ensure sustainable economic development.

Bond behavior is one of the key factors that determine whether recycled aggregates (RA) can be used in concrete structures [7–9]. The findings have been achieved as follows: the bond strength correlates well with the crushing index of RA [10]. The bond strength of recycled concrete with 100% RA is approximately 15% lower than natural aggregates (NA) [11]. Kim et al. found that, the smaller the aggregate size, the higher the bond strength through pull-out test [12]. Early in 1987, Shima et al. proposed the application of bond stress, slip, and reinforcement strain to characterize the bond-slip relationship between concrete and reinforcement [13]. As the research progressed, Kankam obtained the relationship between bond stress and slip through experiments [14], i.e., the τ-s relationship equation. Seara-Paz et al. established a modified expression for predicting the maximum bond strength, considering RA replacement rate and compressive strength [15]. Guizani et al. conducted pull-out tests under monotonic and cyclic loading, respectively, and investigated the influence of the degree of restraint and the number of initial loadings on the test, thereby establishing a bond-slip constitutive model [16]. Gao et al. established the bond strength model between RC and reinforcement based on natural concrete (NC) [17]. Moreover, the model proposed by Hu et al. was obtained with an experiment [18].

(**a**)

(**b**)

Figure 1. Serious construction solid-waste issues. (**a**) Demolition of buildings; (**b**) Tremendous amount of C&DW.

As we all know, freeze-thaw (F-T) damage is part of the main factor that affects the durability of reinforced concrete [19]. Moreover, F-T cycles accelerate the generation and development of concrete cracks, lead to a decrease in bond properties, and are particularly severe in the frozen regions of Northeast China [20]. Hanjari et al. noted that F-T cycles harm bond properties of concrete materials, whether coarse aggregate is NA or RA [21]. Liu et al. points out that, the more RA there is, the more damage caused by F-T cycles [22]. Shi et al. believe the cement paste attached to the surface of RA is the key factor causing the decline in frost resistance [23]. Meanwhile, the experimental results of Reference [18] also support this view. Huaishuai et al. researched the bond performance of fully recycled concrete and various types of steel bars; subsequently, corresponding bond-slip trend curves were given [24]. Wang et al. expressed the bond-slip relationship in terms of the relative dynamic modulus of elasticity loss rate based on the bond-degradation law produced by F-T cycles [25]. In addition, based on the influence of different reinforcement diameters and concrete protective layer thickness on the bond performance, a corresponding empirical model was given by Ren et al. [26]. In summary, most research has been conducted on the negative impact of F-T environments on bond behavior. However, relatively few works have been performed to enhance the bond behavior of recycled concrete and reinforcing steel under F-T conditions.

Studies revealed that fibers have a beneficial effect on the performance of concrete [27]. In actual projects, steel fibers, polypropylene fibers, etc., are utilized to enhance the properties of concrete structures [28]. Especially steel fibers can enhance the frost resistance of concrete [29,30], and with steel fibers, the bond stress of concrete is enhanced by up to 5~20% [31]. Gao et al. investigated the bonding performance of reinforcement with recycled concrete, using RA replacement rate and steel fibers volume content as variables, and finally, a bond-slip model was derived [32]. However, it is mostly used for high-strength and ultra-high-strength concrete, while RC has low in strength, particularly under cold environments, and is more prone to damage, so the role of steel fibers cannot be fully utilized. Fortunately, polypropylene fibers promote the homogeneity of concrete; therefore, the crack and frost resistance were strengthened [33]. Test by Afroughsabet et al. shows that the bond behavior of polypropylene and steel fibers was higher than that of steel fiber [34]. Relatively little research has been conducted, nonetheless, on the bond performance of single-mixed polypropylene fibers with concrete [35], but undoubtedly, polypropylene is a good choice for improving the bonding performance of recycled concrete in cold environments.

Meanwhile, carpets are generally used in households, hotels, and other live and workplaces in China. Moreover, with convenience comes the problem. Each year, more than 13 million tons of waste carpets are produced, of which, mainly polypropylene fibers carpet [36]. In addition to disposal by the landfill, incineration will cause serious pollution to the ecological environment (Figure 2) [37]; regrettably, an economical and environmentally friendly solution has not yet been proposed. It is a thorny problem, with the goal of "carbon neutrality" and "carbon peaking" [38].

(a) (b)

Figure 2. Waste carpets cause environmental problems. (**a**) Waste carpet products; (**b**) Incineration of waste carpets.

The waste carpet is treated, and the recycled fibers (RFs) that are obtained are used in RC; on the one hand, this improves the performance of concrete, but on the other hand, it reduces resource consumption and promotes waste recycling, achieving a win-win situation. Therefore, this paper proposes the concept of recycled fiber recycled concrete (RFRC). Fibers are taken from the waste carpet, firstly; cleaned and disinfected, secondly; and mechanically and manually cut, finally, to acquire fiber segments. Coarse aggregates come from C&DW. Simulating the harsh cold environment of Northeast China, we performed F-T tests (0, 50, 100, 150 cycles) with RA replacement rates of 0, 50%, and 100%; RF volume contents of 0, 0.12%, and 0.24% as variables; and five groups, with 60 specimens in total. The bond behavior between RFRC and reinforcement under F-T cycles was studied. Additionally, local bond-slip tests were conducted to investigate the distribution law of bond stress with RFRC50-12 series. A bond-slip model under F-T condition was established. In this paper, we provide new ideas for the application of waste carpet and C&DW and promote in-depth research on the recycling of the solid waste in cold regions.

2. Materials and Methods

2.1. Materials

In this study, ordinary Portland cement P•O 42.5(Sunnsy Group, Shenyang, China) was used as the cement, which meets GB175-2018 [39]: natural river sand as fine aggregates, fineness modulus 2.7, mud content < 2%, and apparent density 2615 kg/m^3. Two types of coarse aggregates, NA and RA were used: NA from crushed gravel, and RA from the structural laboratory of Shenyang Jianzhu University, original-strength grade C40. Crushed by manual and jaw crusher, cleaned, and sieved; maximum particle size 25 mm, conforms to GB/T 25177-2010 [40] and GB/T 14685-2011 [41]. Figure 3 shows the grading curves of aggregates. Performance indicators are shown in Table 1. Reinforcing steel was used, with 10 and 16 mm. Mechanical properties are shown in Table 2. Mixing water was ordinary tap water.

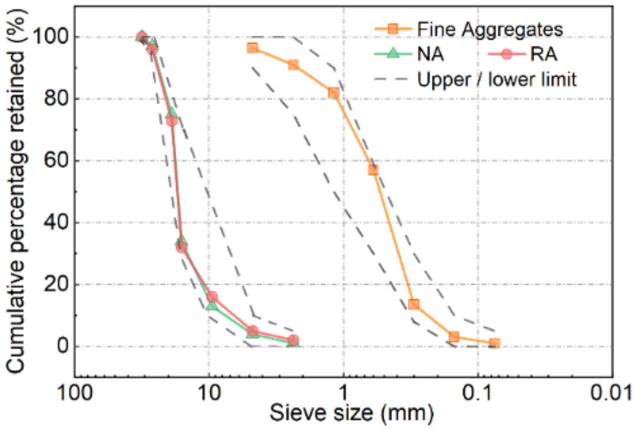

Figure 3. Grading curves of aggregates.

Table 1. Performance index of coarse aggregates.

Type	Apparent Density (kg/m^3)	Bulk Density (kg/m^3)	Water Absorption (%)	Bulk Density (kg/m^3)
Natural	2730	1850	1.12	6.4
Recycled	2460	1275	4.36	17.0

Table 2. Mechanical properties of reinforcement.

Grade	Apparent Density (kg/m^3)	Diameter (mm)	Yield Strength (MPa)	Tensile Strength (MPa)
HRB400	ribbed	10	542	714
HRB400	ribbed	16	566	710

The recycled fibers (RFs) from waste carpet, polypropylene material, density 0.91 kg/m^3, modulus of elasticity 3.5×10^3 MPa, water absorption <0.1%, cleaned and cuts, obtain waste fiber bundles, with length 18 to 20 mm; the preparation process is shown in Figure 4.

Figure 4. Extraction of recycled fibers.

2.2. Concrete Mixture

Due to the old cement mortar attached to the surface of RA, it has a higher water absorption rate. According to Table 1, the water absorption rate of RA is 3.9 times than NA. DG/T J08-2018 [42] stipulates that the mix ratio of recycled concrete should consider the adsorbed water of the aggregates. Being dependent on the standard, every 50% increase of RA is 10 kg/m^3 of additional water approximately. Water absorption of fibers < 0.1%; its influence on water consumption can be ignored. The concrete mixture is shown in Table 3. Specimen preparation process is in Figure 5; the machine was JW350 forced multifunctional mixer (Qianchen Machinery Equipment, Shenyang, China), rotational speed 60 r/min.

Table 3. Concrete mixture.

Notion	RF (%)	Amount of Material (kg·m^{-3}) Cement	Sand	NA	RA
NC [1]	0	390	709	1156	0
RC50	0	390	709	578	578
RC100	0	390	709	0	1156
RFRC50-12	0.12	390	709	578	578
RFRC50-24	0.24	390	709	578	578

[1] NC is natural concrete; RFRC50-12 is RA with 50% and RF 0.12% by volume.

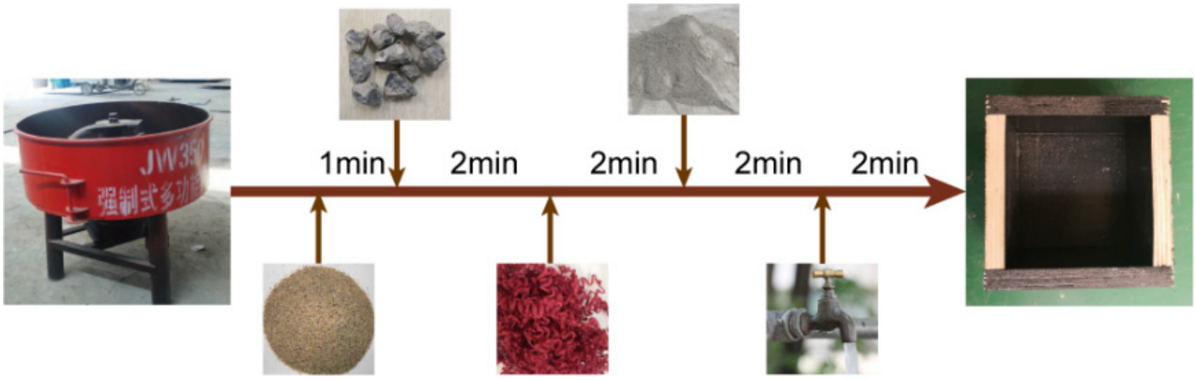

Figure 5. Specimen preparation process.

2.3. Test Specimens

According to the mixture, prepare 100 × 100 × 100 mm pull-out specimen, 5 series, 3 parallel tests per series, 4 F-T cycles (0, 50, 100, 150), 60 in total. Figure 6 shows the details of the specimen: anchorage length 5 times the diameter of reinforcing steel (50 mm). With PVC pipes embedded at each end of the mold, we sealed with paraffin wax to eliminate influence on the test results.

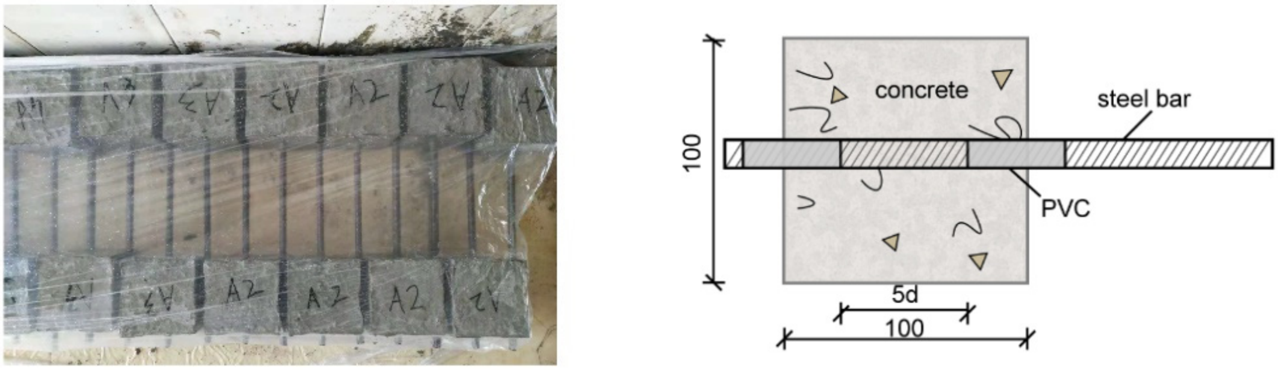

(**a**) (**b**)

Figure 6. Specimens for pull-out tests. (**a**) Specimens; (**b**) Details of the specimen.

Meanwhile, according to the results of F-T cycles, 8 pull-out specimens for bond-stress distribution were made with 100 × 100 × 160 mm. The treatment of reinforcing steel refers to Liu [43] and Tang [44]. Firstly, reinforcing steel is pretreated by cutting along the axis, slotted. Strain gauges inside, spaced 20 mm, 9 pieces. Closed after waterproofing, anchorage length 10 times the diameter of reinforcement (160 mm). Figure 7a shows the steel-bar handling process. Figure 7b shows details of the stress distribution specimen.

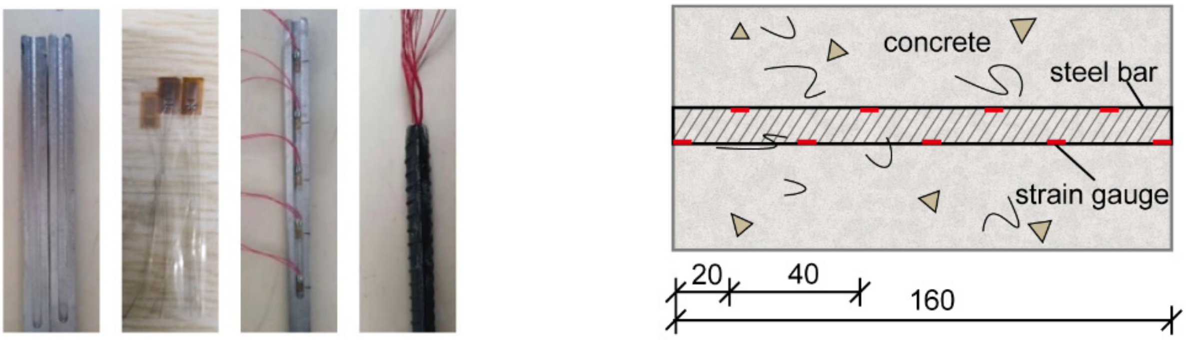

(**a**) (**b**)

Figure 7. Specimens for bond-stress-distribution tests. (**a**) Special treatment for steel bars; (**b**) Details for bond-stress distribution.

2.4. Rapid Freeze-Thaw Cycles Test

Twenty-four hours later, the specimens were demolded and transferred to standard conditions for 23 days of curing. Subsequently, they were immersed in water for 4 days. The test was performed by the quick-freeze method, dependent on the GB/T50082-2009 [45]. The apparatus used a type KDR-V9 concrete rapid freeze-thaw testing machine (Shuzhi Instrument Company, Shenyang, China), as shown in Figure 8. Temperature ranged from −17 to 5 °C, every 50 F-T cycles for one period.

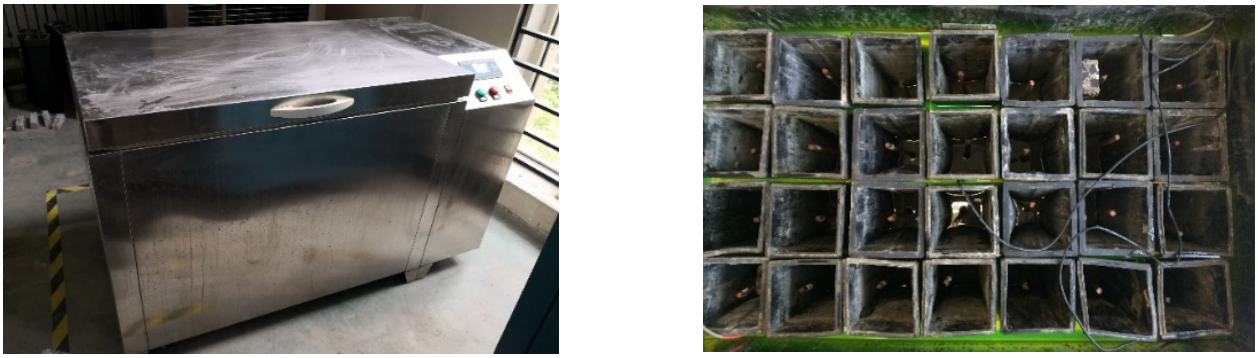

(**a**) (**b**)

Figure 8. Rapid freeze-thaw cycle test of specimens. (**a**) Freeze-thaw testing machine; (**b**) Test chamber.

2.5. Pull-Out Test

The pull-out test with WAW-600C electro-hydraulic servo universal testing machine (Jinan Times Co. Ltd., Jinan, China), as shown in Figure 9, using displacement control method, loading speed 0.3 mm/min. Linear Variable Differential Transformer (LVDT) #1 tests the displacement of loading end. LVDT #2 tests the free end, with automatic data collection. The experiment was carried out with GB/T 50152-2012 [46]; before loading, slowly pressurize the specimen; after the reading of LVDT #1 stable, reset the reading and start. Assume that the bond strength is uniformly distributed over the entire bonded section of steel bar. The bond strength is calculated as in Equation (1):

$$\tau = P/(\pi d l_a) \tag{1}$$

where τ is the bond strength between concrete and reinforcement (MPa), P is pull-out force (kN), d is diameter of reinforcement (mm), and l_a is bond length of reinforcement (mm). The slip of the reinforcement can be calculated by the average value of the loading end (S_1) and free end (S_2), as Equation (2). S_1 and S_2 correspond to the data collected by LVDT #1 and LVDT #2.

$$S = \frac{1}{2}(S_1 + S_2) \quad (2)$$

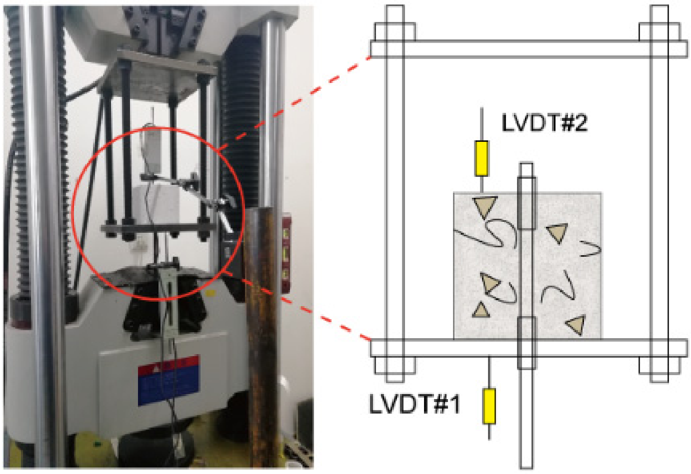

Figure 9. Pull-out test machine of type WAW-600C.

3. Results

3.1. Failure Modes

Changes in apparent morphology can reflect the damage process of RFRC during -T cycles. The morphology for 50, 100, and 150 cycles is shown in Figure 10. At 50 cycles, the peel degree of cement mortar on the surface of the specimen is different; coarse aggregates of the NC, RC50, and RC100 series are exposed. At 100 cycles, the more RA, the more exposure; RC50 coarse aggregates fall off partial, and RC100 edge incomplete. At 150 cycles, a large amount of fine aggregates is spalling, coarse aggregates are exposed obviously, and the surface of the specimen is uneven; RFRC50-12 and RFRC50-24 are less damaged, and RC100 has the most serious damage. The results showed that the -T cycles caused damage to the NC and RC series; the degree was positively correlated with the number of F-T cycles. Furthermore, it is also related to the amount of RA and RF: the greater of the amount of RA, the more serious the damage is, and it should be noted. The addition of RF can improve RC frost resistance to a certain extent.

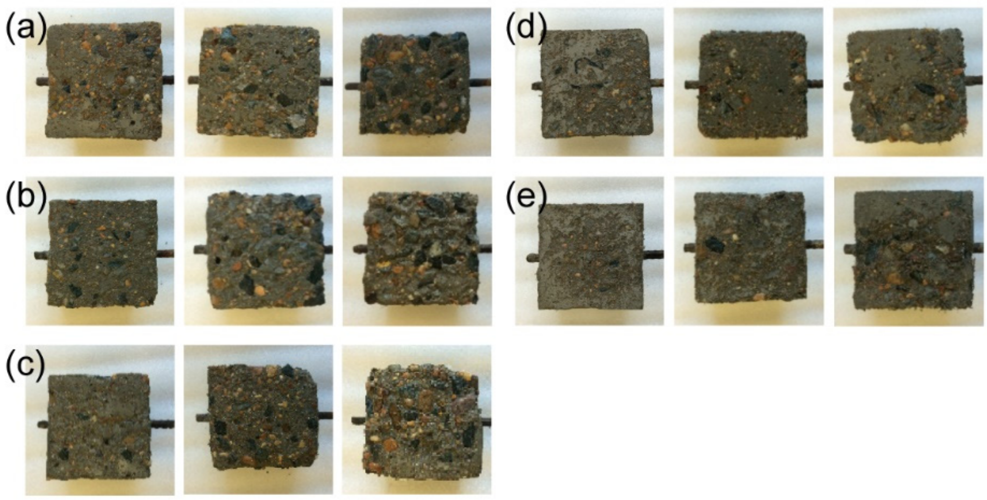

Figure 10. Morphological changes under F–T conditions. (**a**): NC, (**b**): RC50, (**c**): RC100, (**d**): RFRC50-12, (**e**): RFRC50-24.

The pull-out test was be conducted every 50 F-T cycles. The results are shown in Table 4. The data are the average of three specimens, and there are two types of damage:

split and split/pull-out (Figure 11). Split failure produces wide through cracks; the specimen separates into two halves during damaged, with a bursting sound. With split/pull-out failure, there are narrow through cracks, no obvious sound when destroyed, and the specimen can still maintain the integrity after the reinforcement is pulled out. It should be noted that, under 150 F-T cycles, one case of a split occurred in three specimens with the RC100 series, and two cases in the RFRC50-24 series.

Table 4. Experimental results of pull-out test.

Notion	F-T Cycles	Failure Mode	Ultimate Load (kN)	Bond Strength (MPa)	Bond Slip (mm)
NC	0	S-P	30.83	19.63	0.28
	50	S-P	26.09	16.61	0.33
	100	S-P	22.51	14.33	0.38
	150	S-P	16.89	10.75	0.41
RC50	0	S-P	22.7	14.45	0.27
	50	S-P	19.52	12.43	0.31
	100	S-P	15.87	10.1	0.35
	150	S-P	11.62	7.4	0.37
RC100	0	S-P	20.64	13.14	0.29
	50	S-P	17.64	11.23	0.3
	100	S-P	12.82	8.16	0.32
	150	1S + 2S-P	6.31	4.02	0.35
RFRC50-12	0	S-P	21.44	13.65	0.26
	50	S-P	20.75	13.21	0.32
	100	S-P	16.24	10.34	0.34
	150	S-P	12.94	8.24	0.41
RFRC50-24	0	S-P	23.78	15.14	0.25
	50	S-P	21.63	13.77	0.33
	100	S-P	15.41	9.81	0.31
	150	2S + 1S-P	10.81	6.88	0.36

(a)

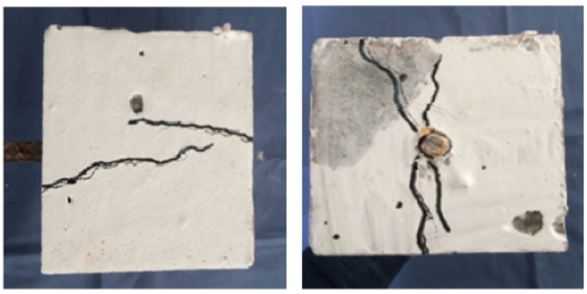

(b)

Figure 11. Failure modes of different types. (**a**) Split; (**b**) Split/pull-out.

3.2. Bond Strength and Bond Slip

Figure 12 presents the relationship between the bond strength and F-T cycles. It can be observed that, as the number of F-T cycles increases, the bond strength gradually decreases. As shown in Figure 12a, the bond-strength loss is 45.24%, 48.79%, and 69.41% for NC, RC50, and RC100 series after 150 F-T cycles. Additionally, with a fixed number of F-T cycles, the bond strength between RC and reinforcement is less than that of the NC series and decreases with the increase of RA. The addition of RA increases the area of the interface transition zone (ITZ) of the material; meanwhile, this part is the weakest area of concrete material performance. Therefore, with the F-T cycles environment, the specimen is more likely to be damaged when subjected to external loads. This is consistent with the failure modes of the specimen. Over 150 F-T cycles later, the reduction in bond strength is lower than 5% for NC and RC50, about 30% for RC100. That is, compared with F-T cycles, the effect of RA on the bond-strength loss is low and negligible at 50% RA replacement.

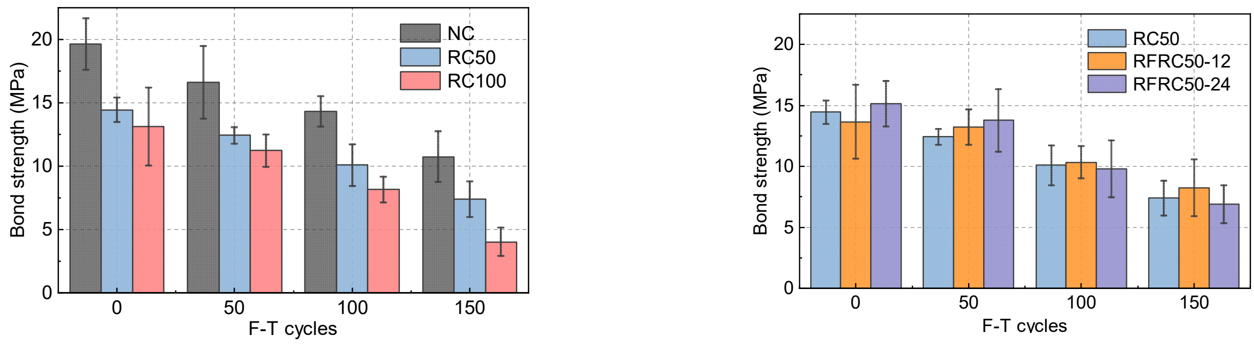

(**a**) (**b**)

Figure 12. Bond strength versus the number of F-T cycles. (**a**) RC series; (**b**) RFRC series.

Figure 12b shows the influence of RF on bond strength under F-T cycles' conditions. After 150 F-T cycles, the bond-strength loss was 48.79%, 39.63%, and 54.56% for the RC50, RFRC50-12, and RFRC50-24 series. Compared to RC50, the bond strength of FRC50-12 increased by 11.35%, while RFRC50-24 increased by 4.78% and decreased by 7.03% before and after cycles. It is shown that the incorporation of RF plays a positive role in the bond behavior of recycled concrete with reinforcement, but it is related to the RF content. A small amount of RF enhances the bonding strength, while excessive RF has a discouraging effect. RF ameliorates the internal structure of recycled concrete, optimizes the mixing of aggregate and mortar, slows down the generation and development of cracks, and plays a certain role in dissipating the energy generated by the force. Moreover, excess RF, which reduces the homogeneity of the mixture, accelerates structural damage in F-T cycles environment, thus resulting in bond-strength reduction.

Figure 13 demonstrates the relationship between slip and F-T cycles. It can be observed that the development trends of curves are similar, and the slip extends with the number of F-T cycles. The reason why is that F-T cycles cause damage to the concrete matrix and reduce the restraining effect of the concrete to the reinforcement. In addition, a fixed number of cycles, increased RA, and decreased slip are related. As shown in Figure 13a, after 150 F-T cycles, the RC50 and RC100 series were reduced by 9.76% and 14.63%, respectively, compared with the NC series. During the loading process, RA between the ribs was more easily crushed, reducing the friction between concrete and reinforcement, which is consistent with the conclusion of [22].

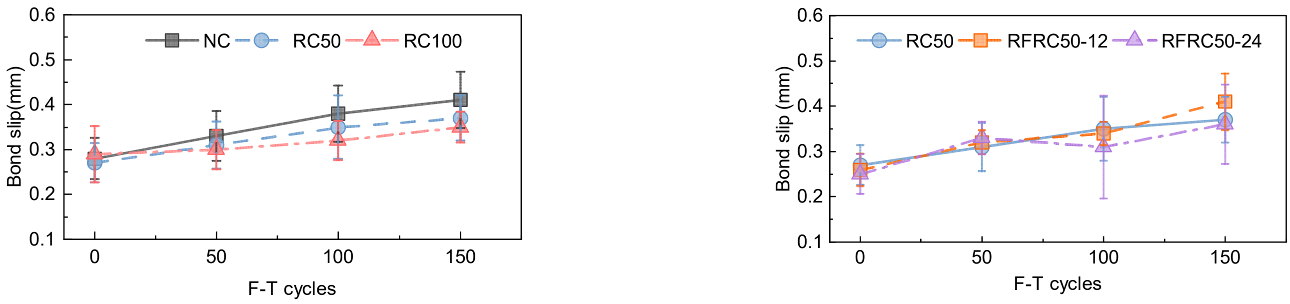

(**a**) (**b**)

Figure 13. Bond slip versus the number of F-T cycles. (**a**) RC series; (**b**) RFRC series.

Figure 13b reflects the influence of RF on slip under F-T cycles conditions. After 150 F-T cycles, the RFRC50-12 slip increased significantly, 13.89% improvement over RC50 series. Whereas the variation of RFRC50-24 slip is not significant. To a certain extent, the addition of RF plays a role in tensile crack resistance and energy consumption but is related to the content.

3.3. Bond-Slip Curves

The bond-slip curves of specimens are shown in Figure 14. Each curve has a similar trend. Overall, the curve can be separated into micro-slip stage, slip stage, extracted stage, descend stage, and residual stage, in accordance with the model of Reference [47]. In the micro-slip stage, pull-out force is quite small, and there is no visible slippage at the free end; the curve varies linearly. At the slip stage, the pull-out force gradually increases, the free end starts to slide, and the curve grows non-linearly. At the pull-out stage, as the force grows to a certain value, the peak strength appears; subsequently, the specimen is damaged, the curve enters descend stage, and the peak strength decreases speedily. In the residual stage, the bond strength decreases slowly and remains stable. It should be noted that, after the F-T cycles, RFRC50-24 failure modes showed split and pull-out.

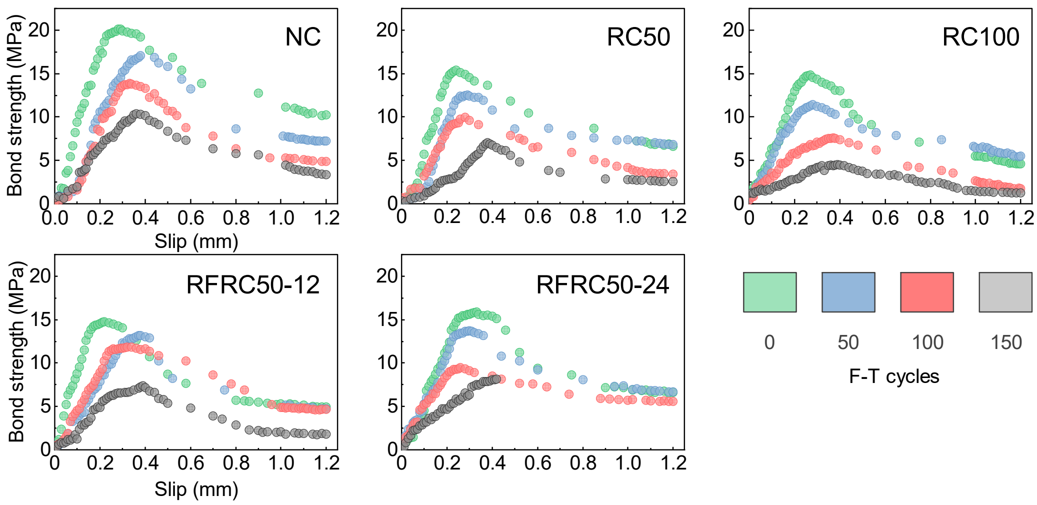

Figure 14. Bond-slip curves of each series under freeze-thaw cycles.

Figure 15 shows the influence of RA on the bond-slip curve under F-T conditions. The curve RC is lower than NC. The more RA there is, the flatter the curve is, as is consistent with the conclusion of the literature [48]. In Figure 15a, we can see that there was no remarkable difference between the curves in the micro-slip stage before the F-T cycles. In the slip stage, with the RA increases, the elastic modulus of the curve decreases; correspondingly, the bond strength decreases. In the slip stage, the difference between curves becomes more significant; the residual strength was 50.87%, 43.04%, and 31.01% of the ultimate strength, respectively. After 150 F-T cycles, each curve becomes flat, as shown in Figure 15b. The percentage of residual strength decreased by 18.98%, 6.77%, and 3.96%. That is, the damage of the NC series' residual strength by F-T cycles is relatively obvious.

The effect of RF content on the bond-slip curve is illustrated in Figure 16. Before the F-T cycles, the development trend of the curve is not much different, but after the F-T cycles, RFRC50-24 damage is the most significant; even the failure mode changes, while RFRC50-12 had good bond behavior.

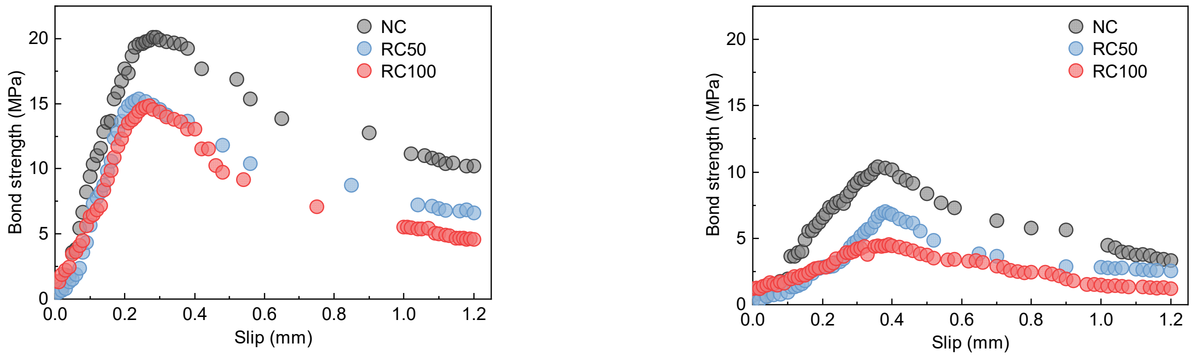

(**a**) (**b**)

Figure 15. Bond-slip curves of different recycled aggregates replacement rates. (**a**) before F-T cycles; (**b**) 150 F-T cycles.

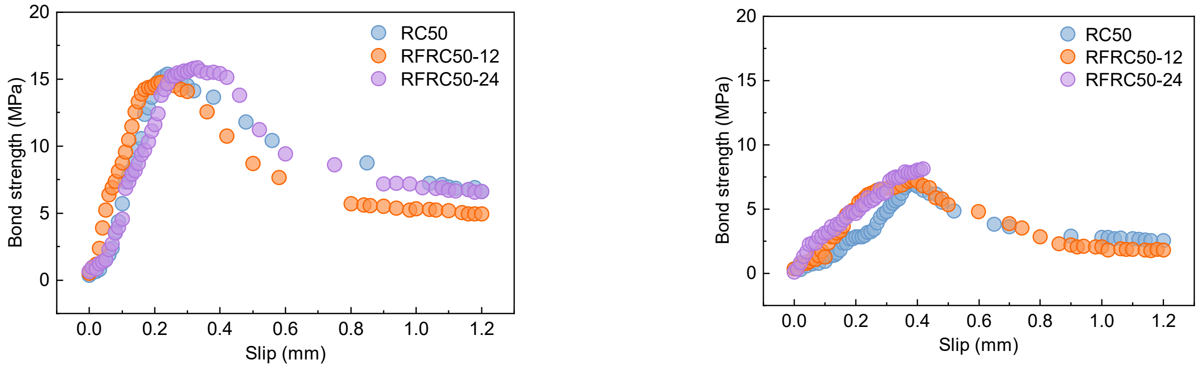

(**a**) (**b**)

Figure 16. Bond-slip curves of different recycled fibers' volume content. (**a**) before F-T cycles; (**b**) 150 F-T cycles.

3.4. Bond Stress Distribution

Take RFRC50-12 series for the bond-stress distribution test under F-T cycles conditions and NC as a control test. Since the bond stress cannot be obtained directly through experiments, it is hypothesized that the stress is uniformly distributed. The stress-equilibrium conditions of the reinforcement are shown in Figure 17, and the bond stress is calculated as follows.

$$\tau = \frac{dP}{\pi ddx} = \frac{d\sigma_s \cdot A_s}{\pi ddx} = \frac{E_s \cdot A_s}{\pi d} \cdot \frac{d\varepsilon_s}{d_s} \tag{3}$$

where σ_s is the tensile stress, dx is the length of the isolated body, and ε_s is the tensile strain. For the convenience of calculation, Equation (4) is mostly utilized to simplify the bond stress of $\tau(x)$ along the anchoring length, *la*.

$$\tau = \frac{Es \cdot A_s}{\pi d} \cdot \frac{\Delta\varepsilon_s}{\Delta x_i} = \frac{E_s \cdot A_s}{\pi d} \cdot \frac{(\varepsilon_j - \varepsilon_{j+1})}{\Delta x_i} = \frac{P_j - P_{j+1}}{\pi d \Delta x_i} \tag{4}$$

where Δx_i is the distance between the two measuring points of the i section; ε_j and ε_{j+1} are the strains of the steel bars at the j and $j+1$; and P_j and P_{j+1} are the tensile force at the j and $j+1$.

Figure 18 shows the bond-stress-distribution curve of RFRC50-12 before and after the F-T cycles. The bond stress is not uniformly distributed throughout the anchorage section, and with the increase of the pull-out force, the stress peak appears in the middle of the bonding area in the curve. At the beginning of loading, there is a negligible difference in bond stress at each position, and as the load increases, the peak point starts to be prominent, and the location does not change with the increase of load. The reason is that the bond stress in this region plays a key role in the load transfer process, and the increase in load does not change this state. Compared with the free end, the bond stress near the loading end increases significantly. Because the loading end is loaded first and then transferred to the free end, while the main bond stress is carried by the intermediate region less bond is transferred to the free end, there is slow growth for the bond stress in this region.

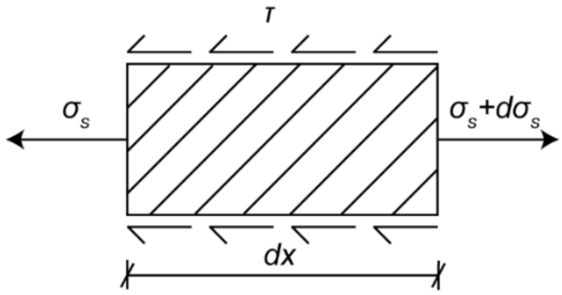

Figure 17. Stress-balance condition of steel bar.

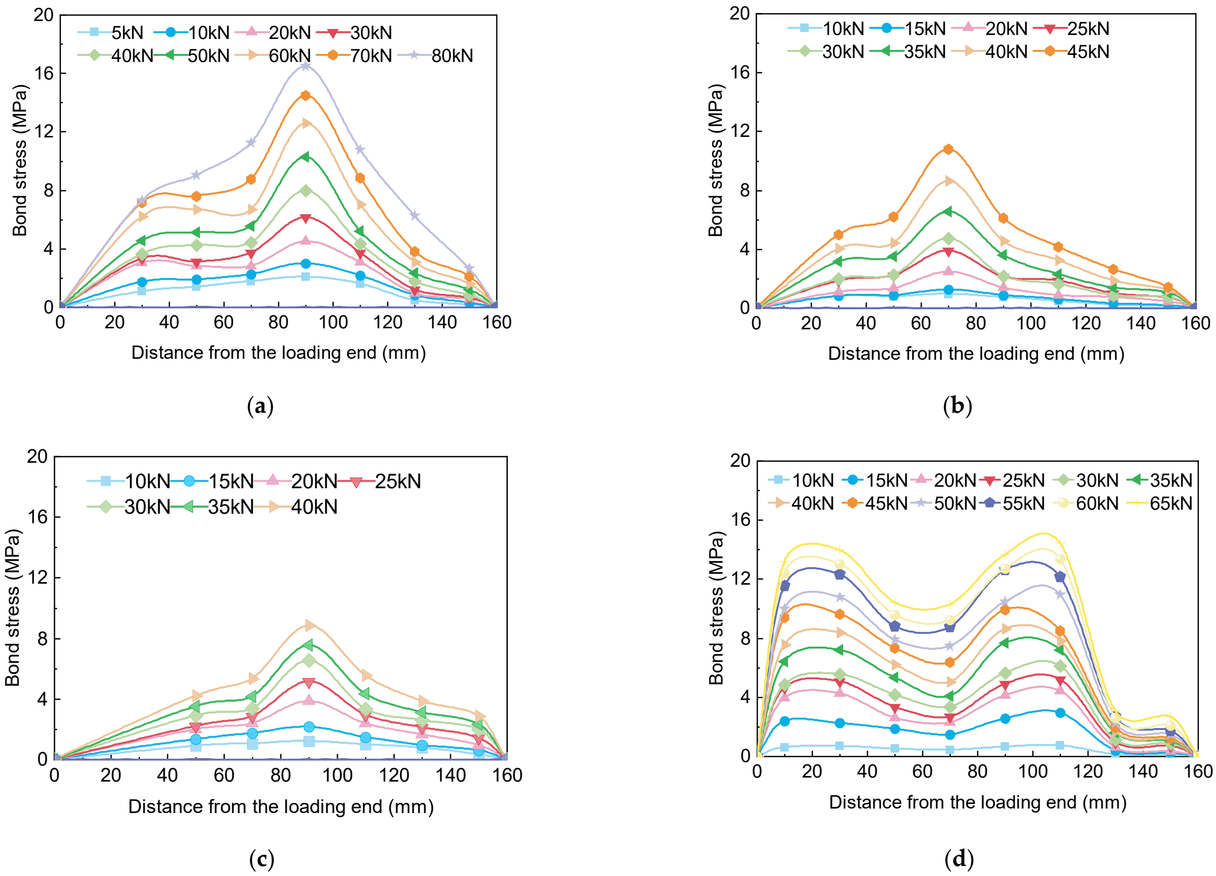

Figure 18. Bondstress distribution along the embedded length. (**a**) RFRC5012-0 cycle; (**b**) RFRC501250 cycles; (**c**) RFRC5012100 cycles; (**d**) NC50 cycles.

The F-T cycles changed the position of the peak point, as it shifted in the direction of the loading end. The reason may be that the specimen can only be fixed in the direction of F-T cycles; as the test proceeds, the loading end of the F-T damage becomes more serious, so the peak position is shifted. The higher the number of F-T cycles, the more dramatic the decrease in peak bond stress. That is, F-T cycles cause internal damage to the RFRC, and the more serious the damage, the more noticeable the decrease in bonding performance.

When the average bond stress is the same, the more uniform the distribution of bond stress, indicating that the utilization rate of bond strength is higher and the ductility is better. To verify the inhomogeneity of the RA to improve the bond stress, this paper introduces μ_1, μ_2, and μ_3 bondstress inhomogeneity coefficients for analysis, and they are calculated as follows.

$$\mu_1 = \frac{\tau_{max}}{\tau_{min}} \tag{5}$$

$$\mu_2 = \frac{\tau_{max}}{\tau_{Av}} \tag{6}$$

$$\mu_3 = \frac{\mu_1 + \mu_2}{2} \tag{7}$$

where τ_{max}, τ_{min}, and τ_{av} are the maximum, minimum, and average bond stress generated under the ultimate load. The closer μ_3 is to 1, the more uniform the bondstress distribution is. The μ_3 of each specimen is illustrated in Figure 19. The μ_3 increases as the number of F–T cycles increases. That is, F–T damage is a gradual accumulation process. The more F–T cycles there are, the more serious the damage and the more uneven the bond-stress distribution. Under the same conditions, RFRC50-12 is higher than NC. This indicates that the addition of RA also improves the inhomogeneity of the material.

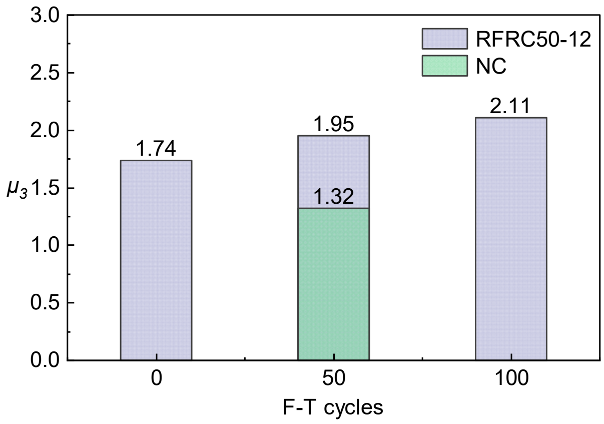

Figure 19. Coefficient of uniformity of bond stress of specimens.

3.5. Freeze-Thaw Damage Mechanism of Bond Stress

The bond stress between concrete and reinforcement is composed of a chemical adhesive force, friction resistance, and mechanical interaction force. Initially, F-T damage acts only on the outer surface of the concrete. With the increase of F-T cycles, cracks are generated in the concrete, thus weakening the restraint effect of the concrete on the internal steel bars and reducing the bond stress. Once the number of F-T cycles reaches a particular value, F-T cracks appear on the interface between concrete and reinforcement, destroying the adhesion and friction forces. Moreover, the bonding stress decreases significantly.

The RA has higher water absorption, and compared with the NC series, the RC series has poorer frost resistance and more significant bond-stress loss. In addition, the relative sliding of the reinforcement when it is pulled out causes the spalled concrete, which is scattered on the surface of the reinforcement, to form a “spherical effect”, which increases the friction coefficient and enhances the frictional resistance [1]. RA is easier to crush and easily crushed into powder when subjected to force, thus promoting the relative sliding between concrete and steel bars and reduces friction. At the same time, the loss of mechanical bite force is evident.

The addition of RF does not alter the properties of recycled concrete, but it prevents the generation and development of cracks, as shown in Figure 20; it also has the effect of absorbing energy and enhancing the mix compatibility, thus enhancing the frost resistance of concrete and reducing F-T damage. This complies with fiber spacing theory; that is, at a certain range, the larger the volume of fibers, the smaller the spacing of fiber distribution in the concrete, and the gap between the matrix material is also reduced. In addition, the fibers across the cracks have an inhibitory effect on the development of oblique cracks [49].

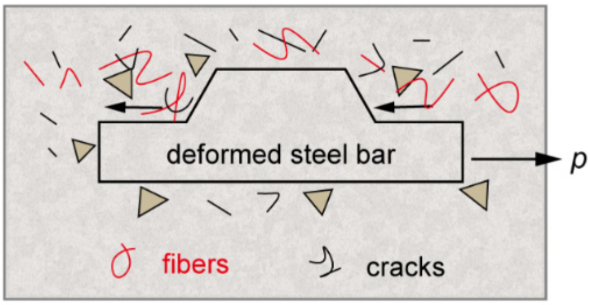

Figure 20. Mechanism of recycled fibers in the pullout process.

In summary, the influence of RA on the bond behavior is primarily concentrated in frictional resistance and mechanical interaction force, while RF is the chemical adhesion force.

3.6. Bond Stress-Slip Model for RFRC

The development trend of the bond-slip curve of each group is the same; it can be simplified into ascending and descending segments. Therefore, a corresponding bond-slip model can be established to determine the bond performance between RFRC and the steel bar interface after F-T cycles. In this paper, depending on the dimensionless parameter bond-slip model proposed by Reference [47], the bond-slip model is shown in Equation (8).

$$\frac{\tau}{\tau_u} = \begin{cases} (S/S_u)^a & S \leqslant S_u \\ \frac{a}{S/S_u+b} & S > S_u \end{cases} \tag{8}$$

where τ_u is ultimate bond stress, and s_u is the ultimate slip. The measured data are fitted according to Equation (8). The fitting results are shown in Table 5. Moreover, Figure 21 shows the comparison between test results and predicted results, which are well fitted, and it is suitable for simulating the bond performance between RFRC and reinforcement.

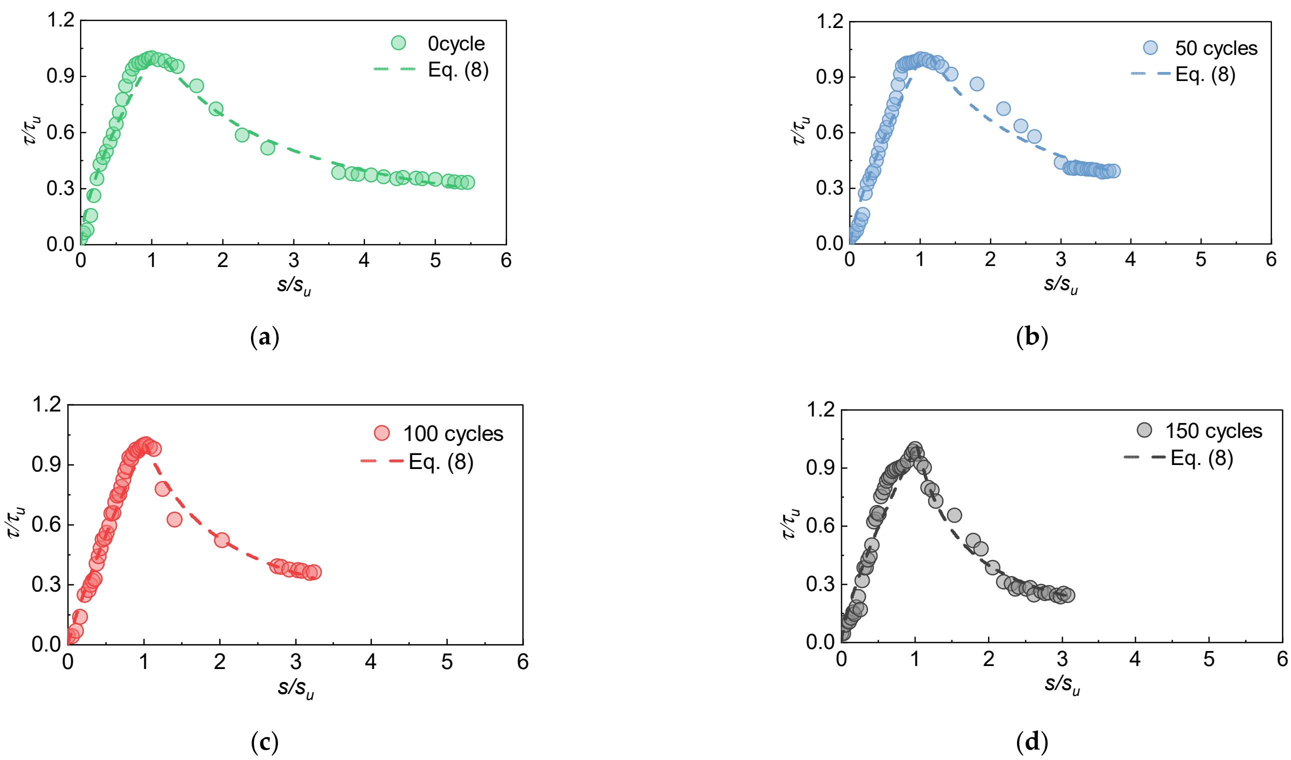

Figure 21. Curvefitting results of RFRC5012 series. (**a**) 0 cycle; (**b**) 50 cycles; (**c**) 100 cycles; (**d**) 150 cycles.

Table 5. Fitting result of the parameter value.

Type	Number of F–T Cycles	Ascending Sections	Descending Sections	
		A	a	b
NC	0	0.74	3.09	2.02
	50	0.98	1.33	0.16
	100	1.16	1.31	0.20
	150	0.90	1.23	0.15
RC50	0	1.09	2.98	1.9
	50	1.23	3.41	2.48
	100	0.90	1.81	0.7
	150	1.51	1.07	0.07
RC100	0	0.84	1.55	0.45
	50	0.71	3.21	2.22
	100	0.58	0.87	−0.2
	150	0.60	0.96	−0.1
RFRC5012	0	0.66	1.86	0.70
	50	0.86	1.11	0.08
	100	0.77	1.65	0.47
	150	0.75	0.64	−0.39
RFRC5024	0	0.80	1.58	0.5
	50	0.79	2.54	1.55
	100	0.67	4.64	3.67
	150	0.66	——	——

4. Conclusions

The bond behavior of RFRC and reinforcement after the F-T cycle was investigated by using the pull-out test. From the experimental results, we determined the major conclusions to be as follows:

(1) The bond strength decreases as the number of F-T cycles increases, whether there are natural or recycled aggregates. For fixed F-T cycles, the bond strength loss of natural aggregates was less than that of recycled aggregate concrete. Compared with F-T cycles, the effect of recycled aggregates' replacement rate on bond strength was not significant; RC50 bond strength is 95% of NC.

(2) The addition of fibers slows down the generation and development of cracks, and it promotes the bond performance under F-T conditions and the optimal dosing of 0.12% in this test.

(3) The NC bond stress distribution is bimodal, the recycled concrete bond-stress distribution is unimodal, that is, the addition of recycled aggregates increases the unevenness of the bond stress. Moreover, the pullout force increases, and the local stress concentration is obvious.

(4) A simplified two-phase bond-slip model is proposed to characterize the bond performance between RFRC and reinforcement after F-T cycles, as it correlates well with the test results.

Author Contributions: Conceptualization, J.Z.; methodology, J.Z. and T.K.; software, Y.L.; validation, D.W. and A.L.; formal analysis, Y.L. and T.K.; investigation, J.Z. and T.K.; resources, J.Z. and T.K.; data curation, Y.L. and D.W.; writing-original draft preparation, Y.L.; writing—review and editing, T.K.; visualization, Y.L. and A.L. All authors have read and agreed to the published version of the manuscript.

Funding: This research was funded by National Natural Science Foundation of China, grant number 52108235 and 51678374 and Liaoning Provincial Department of Education Fund (No. lnqn202003; LT2019011), and Fundamental Research Funds for the Central Universities (No. 300102341511).

Data Availability Statement: Since the experiment was completed with the support of Shenyang Jianzhu University, the data used to support the results of this study are available from the responsible person and the author upon request.

Conflicts of Interest: The authors declare no conflict of interest.

References

1. Wang, F.; Wu, X.; Guo, C.; Song, W. Experimental Study on Bond Strength of Deformed Steel Bars in Recycled Glass Aggregate Concrete. *KSCE J. Civ. Eng.* **2018**, *22*, 3409–3418. [CrossRef]
2. Omrane, M.; Kenai, S.; Kadri, E.-H.; Aït-Mokhtar, A. Performance and Durability of Self Compacting Concrete Using Recycled Concrete Aggregates and Natural Pozzolan. *J. Clean. Prod.* **2017**, *165*, 415–430. [CrossRef]
3. Aslani, F.; Ma, G.; Wan, D.L.Y.; Muselin, G. Development of High-Performance Self-Compacting Concrete Using Waste Recycled Concrete Aggregates and Rubber Granules. *J. Clean. Prod.* **2018**, *182*, 553–566. [CrossRef]
4. Revilla-Cuesta, V.; Skaf, M.; Faleschini, F.; Manso, J.M.; Ortega-López, V. Self-Compacting Concrete Manufactured with Recycled Concrete Aggregate: An Overview. *J. Clean. Prod.* **2020**, *262*, 121362. [CrossRef]
5. Prince, M.J.R.; Singh, B. Bond Behaviour of Normal- and High-Strength Recycled Aggregate Concrete. *Struct. Concr.* **2015**, *16*, 56–70. [CrossRef]
6. Han, Y.; Yang, Z.; Ding, T.; Xiao, J. Environmental and Economic Assessment on 3D Printed Buildings with Recycled Concrete. *J. Clean. Prod.* **2021**, *278*, 123884. [CrossRef]
7. Kim, S.-W.; Yun, H.-D.; Park, W.-S.; Jang, Y.-I. Bond Strength Prediction for Deformed Steel Rebar Embedded in Recycled Coarse Aggregate Concrete. *Mater. Des.* **2015**, *83*, 257–269. [CrossRef]
8. Arezoumandi, M.; Looney, T.J.; Volz, J.S. Effect of Fly Ash Replacement Level on the Bond Strength of Reinforcing Steel in Concrete Beams. *J. Clean. Prod.* **2015**, *87*, 745–751. [CrossRef]
9. Ma, Y.; Guo, Z.; Wang, L.; Zhang, J. Experimental Investigation of Corrosion Effect on Bond Behavior between Reinforcing Bar and Concrete. *Constr. Build. Mater.* **2017**, *152*, 240–249. [CrossRef]
10. Butler, L.; West, J.; Tighe, S. The Effect of Recycled Concrete Aggregate Properties on the Bond Strength between RCA Concrete and Steel Reinforcement. *Cem. Concr. Res.* **2011**, *41*, 1037–1049. [CrossRef]
11. Cao, F.B.; Li, F.Y. Coarse Aggregate Replacement Ratio on the Properties of Recycled Concrete Bonding Effect. *Adv. Mater. Res.* **2014**, *926–930*, 533–536. [CrossRef]
12. Kim, S.-W.; Yun, H.-D. Evaluation of the Bond Behavior of Steel Reinforcing Bars in Recycled Fine Aggregate Concrete. *Cem. Concr. Compos.* **2014**, *46*, 8–18. [CrossRef]
13. Shima, H.; Chou, L.-L.; Okamura, H. Micro and Macro Models for Bond in Reinforced Concrete. *J. Fac. Eng.* **1987**, *39*, 133–194.
14. Kankam, C.K. Relationship of Bond Stress, Steel Stress, and Slip in Reinforced Concrete. *J. Struct. Eng.* **1997**, *123*, 79–85. [CrossRef]
15. Seara-Paz, S.; González-Fonteboa, B.; Eiras-López, J.; Herrador, M.F. Bond Behavior between Steel Reinforcement and Recycled Concrete. *Mater. Struct.* **2014**, *47*, 323–334. [CrossRef]
16. Guizani, L.; Chaallal, O.; Mousavi, S.S. Local Bond Stress-Slip Model for Reinforced Concrete Joints and Anchorages with Moderate Confinement. *Can. J. Civ. Eng.* **2017**, *44*, 201–211. [CrossRef]
17. Gao, X.; Li, N.; Ren, X. Analytic Solution for the Bond Stress-Slip Relationship between Rebar and Concrete. *Constr. Build. Mater.* **2019**, *197*, 385–397. [CrossRef]
18. Hu, X.; Peng, G.; Niu, D.; Zhao, N. Bond Characteristics of Deformed Steel Bar in Early-Age Frozen Concrete during Service Period. *Eng. Struct.* **2019**, *197*, 109438. [CrossRef]
19. Pei, P.; Zheng, S.; Zhang, Y.; Dong, L. Overview on the Bonding of Reinforced Concrete under Pristine, Corrosive and Freeze-Thaw Conditions. *J. Adhes. Sci. Technol.* **2019**, *33*, 761–789. [CrossRef]
20. Shang, H.; Zhao, T.; Cao, W. Bond Behavior between Steel Bar and Recycled Aggregate Concrete after Freeze–Thaw Cycles. *Cold Reg. Sci. Technol.* **2015**, *118*, 38–44. [CrossRef]
21. Hanjari, K.Z.; Utgenannt, P.; Lundgren, K. Experimental Study of the Material and Bond Properties of Frost-Damaged Concrete. *Cem. Concr. Res.* **2011**, *41*, 244–254. [CrossRef]
22. Liu, X.; Liu, Y.; Wu, T.; Wei, H. Bond-Slip Properties between Lightweight Aggregate Concrete and Rebar. *Constr. Build. Mater.* **2020**, *255*, 119355. [CrossRef]
23. Shi, J.; Zhu, H.; Wu, Z.; Seracino, R.; Wu, G. Bond Behavior between Basalt Fiber–Reinforced Polymer Sheet and Concrete Substrate under the Coupled Effects of Freeze-Thaw Cycling and Sustained Load. *J. Compos. Constr.* **2013**, *17*, 530–542. [CrossRef]
24. Huaishuai, S.; Zhiheng, W.; Peng, Z.; Tiejun, Z.; Guoxi, F.; Guosheng, R. Bond Behavior of Steel Bar in Air-Entrained RCAC in Fresh Water and Sea Water after Fast Freeze-Thaw Cycles. *Cold Reg. Sci. Technol.* **2017**, *135*, 90–96. [CrossRef]
25. Wang, Z.; Zeng, Q.; Wang, L.; Yao, Y.; Li, K. Corrosion of Rebar in Concrete under Cyclic Freeze–Thaw and Chloride Salt Action. *Constr. Build. Mater.* **2014**, *53*, 40–47. [CrossRef]
26. Ren, G.; Shang, H.; Zhang, P.; Zhao, T. Bond Behaviour of Reinforced Recycled Concrete after Rapid Freezing-Thawing Cycles. *Cold Reg. Sci. Technol.* **2019**, *157*, 133–138. [CrossRef]
27. Zareei, S.A.; Ameri, F.; Bahrami, N.; Shoaei, P.; Musaeei, H.R.; Nurian, F. Green High Strength Concrete Containing Recycled Waste Ceramic Aggregates and Waste Carpet Fibers: Mechanical, Durability, and Microstructural Properties. *J. Build. Eng.* **2019**, *26*, 100914. [CrossRef]

28. Wu, X.; Zhou, J.; Kang, T.; Wang, F.; Ding, X.; Wang, S. Laboratory Investigation on the Shrinkage Cracking of Waste Fiber-Reinforced Recycled Aggregate Concrete. *Materials* **2019**, *12*, 1196. [CrossRef] [PubMed]
29. Liu, Z.; Lu, Y.; Li, S.; Zong, S.; Yi, S. Flexural Behavior of Steel Fiber Reinforced Self-Stressing Recycled Aggregate Concrete-Filled Steel Tube. *J. Clean. Prod.* **2020**, *274*, 122724. [CrossRef]
30. Merli, R.; Preziosi, M.; Acampora, A.; Lucchetti, M.C.; Petrucci, E. Recycled Fibers in Reinforced Concrete: A Systematic Literature Review. *J. Clean. Prod.* **2020**, *248*, 119207. [CrossRef]
31. Domski, J.; Katzer, J.; Zakrzewski, M.; Ponikiewski, T. Comparison of the Mechanical Characteristics of Engineered and Waste Steel Fiber Used as Reinforcement for Concrete. *J. Clean. Prod.* **2017**, *158*, 18–28. [CrossRef]
32. Gao, D.; Yan, H.; Fang, D.; Yang, L. Bond Strength and Prediction Model for Deformed Bar Embedded in Hybrid Fiber Reinforced Recycled Aggregate Concrete. *Constr. Build. Mater.* **2020**, *265*, 120337. [CrossRef]
33. Khan, M.; Ali, M. Effectiveness of Hair and Wave Polypropylene Fibers for Concrete Roads. *Constr. Build. Mater.* **2018**, *166*, 581–591. [CrossRef]
34. Afroughsabet, V.; Biolzi, L.; Monteiro, P.J.M. The Effect of Steel and Polypropylene Fibers on the Chloride Diffusivity and Drying Shrinkage of High-Strength Concrete. *Compos. Part B Eng.* **2018**, *139*, 84–96. [CrossRef]
35. Di Maida, P.; Radi, E.; Sciancalepore, C.; Bondioli, F. Pullout Behavior of Polypropylene Macro-Synthetic Fibers Treated with Nano-Silica. *Constr. Build. Mater.* **2015**, *82*, 39–44. [CrossRef]
36. Zhou, J.; Kang, T.; Wang, F. The Permeability of Waste Fiber Recycled Concrete. *Mater. Sci.* **2019**, *26*, 210–217. [CrossRef]
37. Mohammadhosseini, H.; Awal, A.S.M.A.; Yatim, J.B.M. The Impact Resistance and Mechanical Properties of Concrete Reinforced with Waste Polypropylene Carpet Fibres. *Constr. Build. Mater.* **2017**, *143*, 147–157. [CrossRef]
38. Kurad, R.; Silvestre, J.D.; de Brito, J.; Ahmed, H. Effect of Incorporation of High Volume of Recycled Concrete Aggregates and Fly Ash on the Strength and Global Warming Potential of Concrete. *J. Clean. Prod.* **2017**, *166*, 485–502. [CrossRef]
39. Chinese National Standard. *GB175-2018 Common Portland Cement*; Standards Press of China: Beijing, China, 2018. (In Chinese)
40. Chinese National Standard. *GB/T 25177-2010 Recycled Coarse Aggregate for Concrete*; Standards Press of China: Beijing, China, 2010. (In Chinese)
41. Chinese National Standard. *GB/T 14685-2011 Pebble and Crushed Stone for Construction*; Standards Press of China: Beijing, China, 2011. (In Chinese)
42. Chinese Local Standard. *DG/T J08-2018 Technical Specification for the Application of Recycled Concrete*; Standards Press of China: Shanghai, China, 2018. (In Chinese)
43. Liu, S.; Du, M.; Tian, Y.; Wang, X.; Sun, G. Bond Behavior of Reinforced Concrete Considering Freeze–Thaw Cycles and Corrosion of Stirrups. *Materials* **2021**, *14*, 4732. [CrossRef] [PubMed]
44. Tang, C.-W. Modeling Uniaxial Bond Stress–Slip Behavior of Reinforcing Bars Embedded in Concrete with Different Strengths. *Materials* **2021**, *14*, 783. [CrossRef]
45. Chinese National Standard. *GB/T50082-2009 Standard for Test Methods of Long-Term Performance and Durability of Ordinary Concrete*; Standards Press of China: Beijing, China, 2009. (In Chinese)
46. Chinese National Standard. *GB/T 50152-2012 Standard for Test Method of Concrete Structures*; Standards Press of China: Beijing, China, 2012. (In Chinese)
47. Xiao, J.; Falkner, H. Bond Behaviour between Recycled Aggregate Concrete and Steel Rebars. *Constr. Build. Mater.* **2007**, *21*, 395–401. [CrossRef]
48. Prince, M.J.R.; Singh, B. Bond Behaviour of Deformed Steel Bars Embedded in Recycled Aggregate Concrete. *Constr. Build. Mater.* **2013**, *49*, 852–862. [CrossRef]
49. Shao, Y.; Lefort, T.; Moras, S.; Rodriguez, D. Studies on Concrete Containing Ground Waste Glass. *Cem. Concr. Res.* **2000**, *30*, 91–100. [CrossRef]